Investigation of Die Stress Profiles During Powder Compaction Using Instrumented Die

Sung-Tae Hong, Yuri Hovanski, Curt A. Lavender, and K. Scott Weil

(Submitted November 20, 2007; in revised form February 28, 2008)

The die stress profiles during compaction of commercially pure titanium (Ti) and commercial lubricated iron (Fe) powders were experimentally investigated using an instrumented die. The die was designed to simulate double-action pressing, and a detailed stress profile was measured along the height of the die using multiple custom-made strain gage pins. The stress history shows that residual stress remained in the die in the radial direction after the axial compaction stress was removed from the powder. Also, the stress profile at the maximum axial stress and the residual stress profile were observed to be symmetric across the height of the compact for both powders, but both have a unique shape for each powder. For both the stress profile at the maximum axial stress and the residual stress profile, the unlubricated Ti powder produced a much higher radial stress at the center of the compact with a steep pressure gradient on both top and bottom of the compact, while the lubricated Fe powder produced a rather uniform radial stress distribution along the height of the compact.

1. Introduction

Titanium (Ti) and its alloys have mechanical and physical properties attractive to various industrial applications. While Ti is generally expensive, properties such as excellent corrosion resistance and a high strength-to-weight ratio continue to make this material attractive to many industries (Ref 1). The high material cost in the manufacture of Ti components is unfortunately only further exacerbated by difficulties associated with low weight-yield conventional manufacturing processes such as forging and machining. One way to overcome the problem of high Ti component cost is the use of a near-net shape process such as powder metallurgy (PM) (Ref 2). Among the various manufacturing techniques of PM product, uniaxial die compaction, or simply die compaction, is a quite commonly used method.

The friction on the die wall is one of the dominant parameters in the manufacture of PM product via die compaction (Ref 3-7). A high die wall friction alone results in numerous problematic effects ranging from nonhomogeneous green density in the compact to visible distortion of the

Sung-Tae Hong, Yuri Hovanski, Curt A. Lavender, and **K. Scott Weil**, Pacific Northwest National Laboratory, P.O. Box 999, Richland, WA 99352; and **Sung-Tae Hong**, School of Mechanical and Automotive Engineering, University of Ulsan, P.O. Box 18, Ulsan 680-749, Republic of Korea. Contact e-mails: sthong@ulsan.ac.kr and yuri.hovanski@pnl.gov

compacted powder. Die wall friction also increases the ejection force and eventually shortens the die life by die wear and galling. Die wall friction is affected by the interparticle friction of the compacted powder and the friction between the die wall and the powder. The effects of the interparticle friction and the die-wall friction in die compaction of various metallic and nonmetallic powders have been investigated by many researchers (Ref 3-13). Instrumented dies have been used for experimental investigation of friction in powder compaction (Ref 3-8, 10, 12) and can be modified to measure radial stress (Ref 3, 6, 8). Such measurement enables the direct calculation of the friction coefficient at the die wall as a function of the applied pressure at each stage of compaction/ejection without arbitrarily selected parameters for the calculation of the friction coefficient (Ref 4). While this methodology clearly provides an ability to analyze the effects of friction on die compaction, previously designed instrumented dies (Ref 3, 6, 8) had a limited number of radial stress measurement locations. Research presented in this report will show that the die stress profile, i.e., the distribution of the radial stress along the height of the die, varies significantly depending on the properties of a given powder. It is expected that the ejection force is significantly affected by the die stress profile at the final stage of compaction, since the compact should be ejected thorough the die prestressed during the compaction process. Therefore, a complete, or at least more detailed, die stress profile during compaction needs to be measured, especially for Ti power where high particle-die wall friction can shorten the die life.

The results of an investigation of the die stress profile during metal powder compaction using an enhanced instrumented die are reported here. The instrumented die was designed to have an enhanced capacity for radial stress measurement in comparison with that used previously by others (Ref 3, 6, 8). The die was also designed to simulate double-action pressing, which is used almost exclusively in commercial PM to produce better uniformity of green density in the compact. The die stress profiles along the height of the die for commercially pure

(unlubricated) Ti powder and industrial (blended with lubricant) iron (Fe) powders will be presented and discussed.

2. Experiments

2.1 Powder Characterization

The Ti powder used in this study was an unlubricated commercially pure (CP) Ti powder called Hunter Fines (a byproduct of Na reduction of $TiCl_4$) and a standard industrial Fe powder by Hoeganaes (Cinnaminson, NJ) blended with an ethylene bistearamide wax at a mixture of 0.75% by weight. The apparent densities of the Ti powder and the Fe powder used in this research were 0.87 and 2.94 g/cm^3, respectively.

The powder morphology was qualitatively evaluated via scanning electron microscopy (SEM) using a JEOL JSM 5900LV scanning electron microscope. The micrograph of the Ti powder demonstrates the relative low-density, highly agglomerated particulate produced via the Hunter Fines process as shown in Fig. 1(a). The micrograph of the Fe powder, as shown in Fig. 1(b), demonstrates a more densely formulated particulate when compared with the Ti powder in Fig. 1(a) as expected for an atomized powder. As shown in Fig. 1, the Ti powder used in this research maintains a very fine ligament
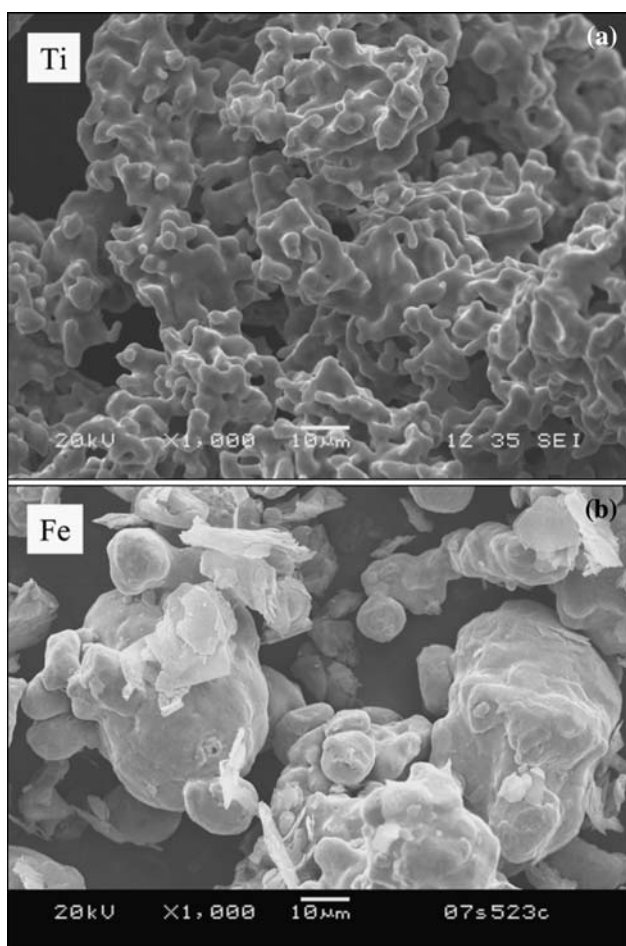

Fig. 1 Representative micrographs of (a) the unlubricated Ti powder and (b) the lubricated Fe powder

structure while its apparent (agglomerated) particle size distribution is similar to that of the Fe powder. The apparent particle size distributions of the powders as determined by screening for the Ti powder and as provided by the manufacturer for the Fe powder are listed in Table 1.

2.2 Enhanced Instrumented Die

An enhanced instrumented die was designed for the measurement of the die stress profile as schematically shown in Fig. 2(a) and included 13 strain gage pin holes machined along the radial direction. The strain gage pin holes were

Table 1 The particle size distributions of the Ti and Fe powders

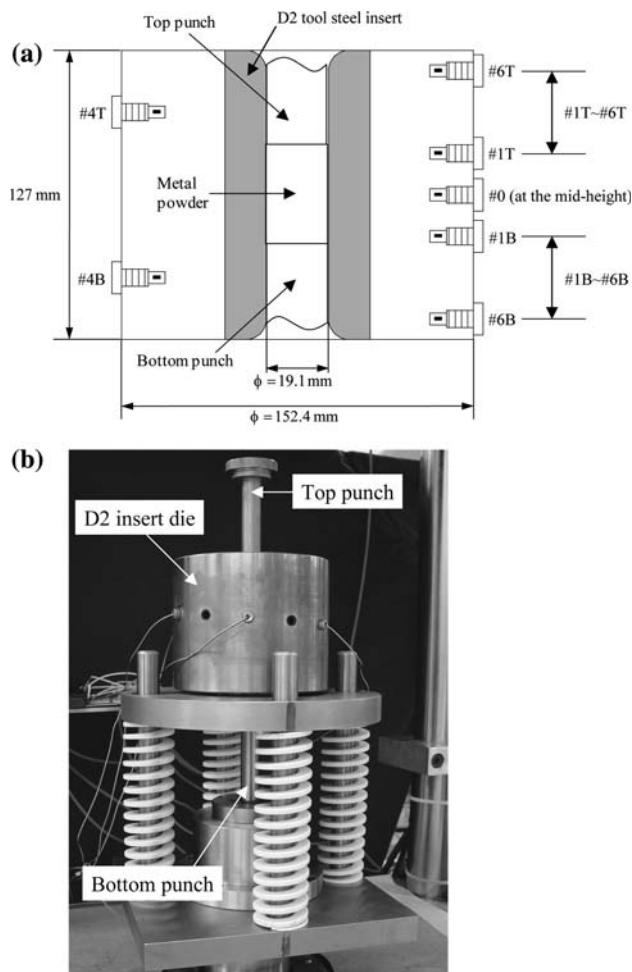| Powder	Sieve distribution (%), μm			
	(+250)	(−250/+150)	(−150/+45)	(−45)
Ti	Trace	36	59	5
Fe	Trace	10	68	22

Fig. 2 (a) A schematic of the enhanced instrumented die: a cross-sectional side view. The strain gage pin holes in the die were located helically at 30° angular increments and 2.54 mm height intervals. (b) The experimental set-up to simulate a double-action pressing. Two strain gage pin holes were left open to clearly show the location of the holes

located helically at 30° angular increments and 2.54 mm height intervals. The enhanced instrumented die was fabricated of 4340 steel with a D2 tool steel insert and matching D2 tool steel punches. Double-action pressing was simulated using four linear springs under the die that allowed the die body to travel downward during pressing effectively simulating double-action pressing as shown in the die schematic of Fig. 2(b). The effectiveness of the dies at simulating double action was validated by monitoring the die body displacement during pressing and it was found that a spring constant of 65.2 kN/m produced nearly ideal double action for the Ti and Fe powders evaluated.

2.3 Data Acquisition and Experimental Procedure

Continuous monitoring of position, load, radial stress, and other less notable conditions was required to facilitate real-time analysis of stress and friction. The applied axial load and the displacement of the top punch were monitored by a load cell and an LVDT on a servo-hydraulic test frame, respectively. An additional LVDT was used to monitor the displacement of the die during compaction and ejection. Thirteen custom-made stainless steel strain gage pins were used to continuously measure the radial stress in the die. In the assembly of a strain gage pin and the die, the strain gage pin was axially constrained between the die wall and a screw with a predrilled hole for wiring as schematically shown in Fig. 3. By this, the radial stress could be determined independently at the location of each stain gage pin. The data acquisition was monitored by an NI-USB 2300 hub at the rate of 100 Hz. The voltage output from the strain gage was conditioned by either Vishay 2300 signal conditioning units or a Daytronix/BCM combination.

The individual conversion of the voltage output of each strain gage to radial stress was accomplished by inducing a nearly hydrostatic pressure inside the die. This nearly hydrostatic pressure condition was induced by compressing an elastomer (silicon rubber) cylinder in the die with a known force. Since elastomeric materials exhibit negligible shear strength in comparison with their bulk modulus (Ref 6), the stress state inside the die can be considered as nearly hydrostatic. The elastomer cylinder was compressed with an axial force (load control) to induce a hydrostatic pressure linearly increasing up to a maximum of 552 MPa while the voltage output of the strain gages was measured as a function of the hydrostatic pressure. The stress at each location was determined from the slope of the voltage output for each strain gage as a function of hydrostatic pressure.

For the compaction of the unlubricated Ti powder, the die was loosely filled with 5 g of the Ti powder to the uncompacted powder height of approximately 20 mm. To achieve similar
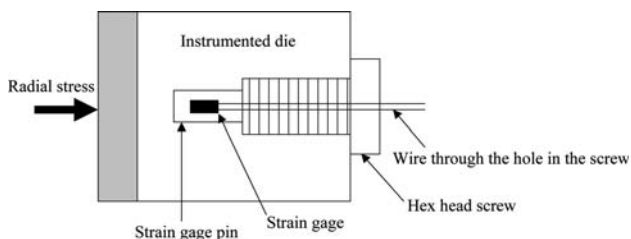

Fig. 3 A schematic of the assembly of a strain gage pin and the enhanced instrumented die

heights of the final compact, 10 g of the lubricated Fe powder was required, filling the die to an approximate height of 12.5 mm. In each experiment, the initial position of the bottom punch was adjusted according to the uncompacted height of the metal powder so that the initial positions of the top and bottom punches were symmetric with respect to the vertical center of the die. During compaction, the top punch moved down with a load control of 4.45 kN/s until the applied load reached the preset maximum load of 160 kN, which corresponds to the axial stress of 552 MPa. Once the applied load reached the preset maximum, the load was held for 5 s (hold phase), and then the top punch was removed from the die, and a circular ring was inserted between the die and the load cell. Finally, the die was pressed down so that the bottom punch ejected the metal powder compact through the top bore of the die (ejection phase).

3. Results and Discussion

Die compaction occurs in four basic phases based on the application of punch force, (1) the compaction phase where the powder is loaded to the predetermined pressing pressure, (2) the hold phase where the maximum force was maintained for 5 s, (3) the unloading phase where the axial force is removed, and (4) the ejection phase where one of the punches is removed and the compact is pushed out of the die. For the die used in this study, a sleeve was manually installed on the top of the die between the unloading and the ejection phase; therefore, there was a brief hold period where the compact was not under axial force. This was the point at which the residual radial stress was determined.

During the compaction phase, the Ti and Fe powders were compacted with the preset maximum axial stress of 552 MPa to green densities approximately 85% and 88%, respectively, compared to the corresponding theoretical values of 4.48 and 7.87 g/cm^3. For both the Ti and Fe powders, the radial stress increased nearly linearly with the axial stress in the compaction phase as shown in the histories of the radial stress at the vertical center of the die as a function of time in Fig. 4(a) and (c), respectively. For the experimental results shown in Fig. 4(a) and (b), the radial stresses at the maximum axial stress for the Ti and Fe powders are 112 and 126 MPa, respectively.

The compact was then held under constant axial stress for 5 s and then unloaded. The axial force then dropped to zero as the top punch was removed from the die and the test set-up was modified for ejection as described above. However, even though the axial stress dropped to zero, a "residual" radial stress existed for both the Ti and Fe powders as shown in Fig. 4(a) and (c). The residual stress induces a frictional resistance force, which must be overcome to eject the compact from the die. The gradual decrease of the radial stress in the ejection phase was reasonable because as ejection continued, the part left the location of stress measurement. However, the gradual change of the ejection stress after the initial peak, as shown in Fig. 4(b) and (d), probably needs more appreciation, even though the change was not pronounced for the Fe powder. This gradual change of the axial ejection stress suggests that the distribution of the residual radial stress along the height of the die was not constant.

The radial stress state in the die at the maximum axial stress showed a fairly symmetric distribution along the height of the compact for both the Ti and Fe powders, although the
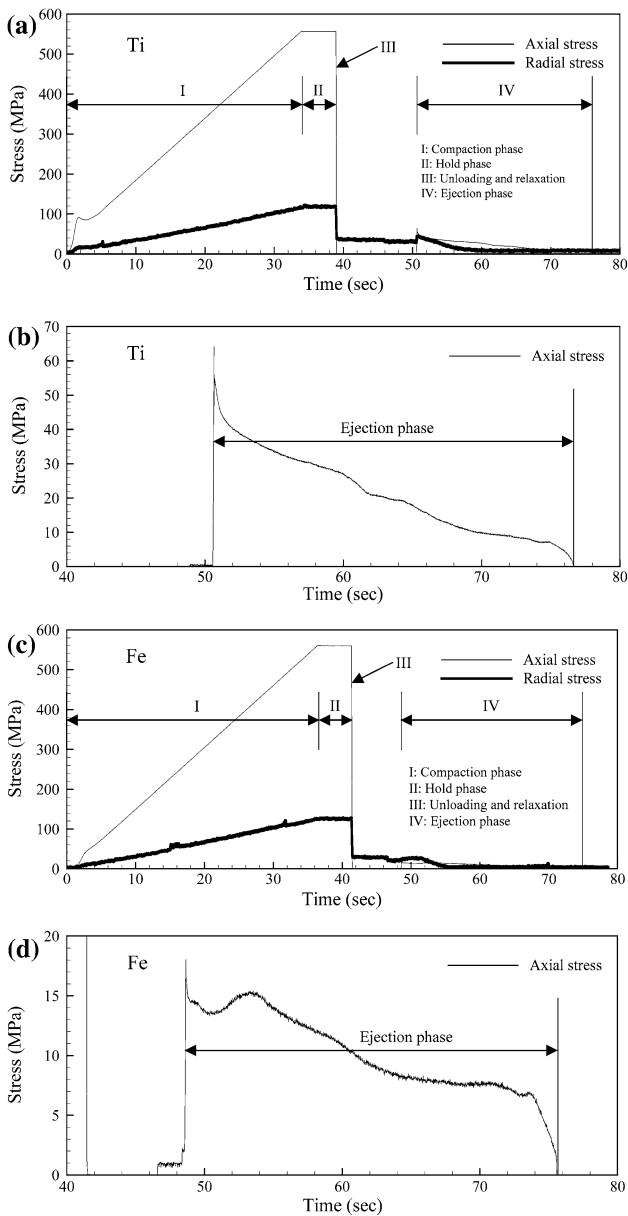
Fig. 4 Typical stress histories for the unlubricated Ti powder: (a) the axial stress and the radial stress at the vertical center of the die; (b) the axial stress in the ejection phase and the lubricated Fe powder; (c) the axial stress and the radial stress at the vertical center of the die; (d) the axial stress in the ejection phase

Fig. 5 (a) Typical profiles of the radial stress at the maximum axial stress for the unlubricated Ti and lubricated Fe powders. (b) Typical profiles of the residual radial stress for the unlubricated Ti and lubricated Fe powders. Note that each tick on the abscissas of (a) and (b) represents the stress measurement location of the die

symmetry for each material varied as shown in Fig. 5(a). The Ti powder produced a much higher radial stress at the center of the compact with a steep pressure gradient on either side, while the Fe powder produced a rather uniform radial stress distribution along the height of the compact. The more uniform radial stress distribution along the height of the Fe compact during compaction may suggest more uniform density in the Fe green compact than in the Ti green compact. Also, the residual stress profile for the Ti powder varied along the height of the die (also the compact) while the residual stress profile for the Fe powder was rather uniform along the height of the die (also the compact) as shown in Fig. 5(b). This may explain why the axial stress varied more in the ejection phase of the Ti compact, as shown in Fig. 4(a) and (b). Note that each tick on the abscissas
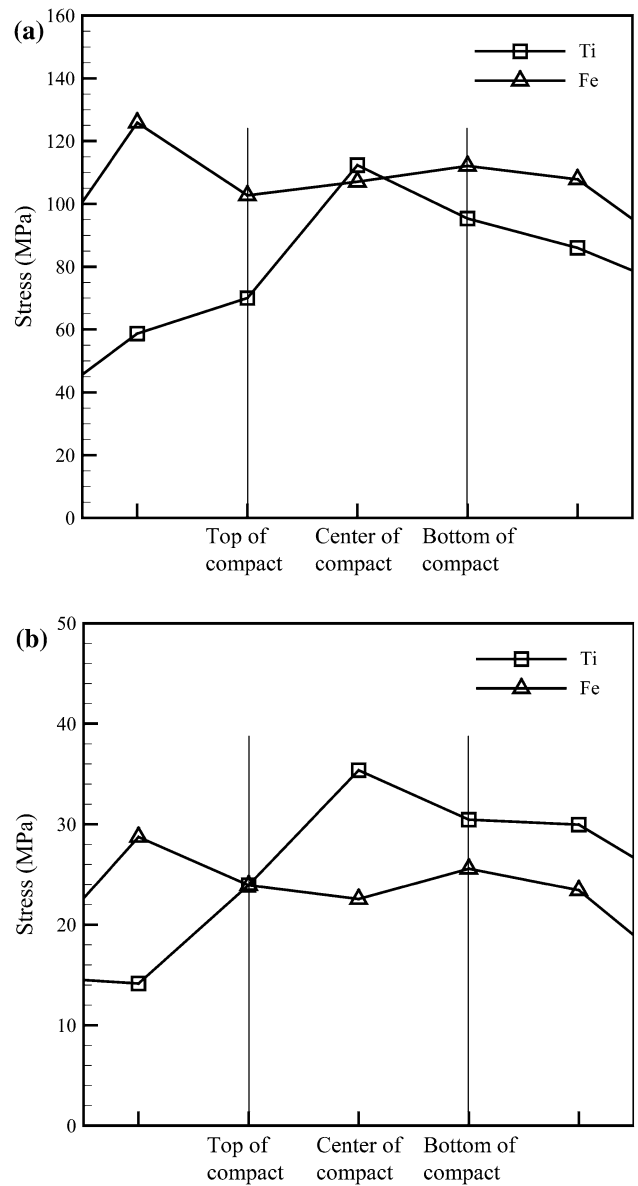
of Fig. 5(a) and (b) represents the stress measurement location of the die.

Die wall frictional coefficient μ can be calculated from a variety of relationships such as the following (Ref 6):

$$\frac{F_T}{F_B} = \exp\left(\frac{4K\mu H}{D}\right) \qquad (Eq\ 1)$$

where F_T is the force on the top punch, F_B is the force on the bottom punch, D is the diameter of the die bore, H is the instantaneous height of the compacted powder, and K is the ratio of the radial stress to the axial stress. The force on the bottom punch, F_B, in the compaction phase was calculated using force equilibrium. With four springs, which have a same spring constant k, the force equilibrium can be simply written as

Table 2 The average frictional coefficient μ at the limit axial stress, and the maximum axial ejection stress for the unlubricated Ti and lubricated Fe powders

Powder	Average frictional coefficient at the maximum axial stress of 552 MPa	Maximum axial ejection stress, MPa
Ti	0.072	64.1
Fe	0.028	26.8

$$F_B = F_T - 4kd_S \qquad \text{(Eq 2)}$$

where d_S is the displacement of the spring, which equals the displacement of the die. Substituting Eq 2 into Eq 1 gives the powder-die wall frictional coefficient μ as

$$\mu = \frac{D}{4KH} \ln\left(\frac{F_T}{F_T - 4kd_S}\right) \qquad \text{(Eq 3)}$$

For the calculation of the frictional coefficient using Eq 3, the parameter K was calculated using the radial stress at the center of the compacted powder. At the same maximum axial stress, the frictional coefficient μ of the Ti powder was quite different from that of the Fe powder as listed in Table 2. As could be expected, the unlubricated Ti powder showed a significantly higher frictional coefficient and consequently a significantly higher ejection stress than the lubricated Fe powder. Note that the results listed in Table 2 are the average values of at least three experimental results for each powder.

4. Conclusion

The die stress profiles during compaction of the unlubricated Ti and lubricated Fe powders were experimentally investigated using an instrumented die. The die was designed to simulate double-action pressing, and a detailed stress profile was measured along the height of the die and the powder compact using multiple strain gage pins.

The stress history of the die shows that residual stress still existed in the radial direction even after the axial stress (pressing force) was removed for both the Ti and Fe powders. The symmetry of the radial stress profiles found in both powders is indicative of stress profiles modeled for other double-acting presses, however the die used for this study was able to predict a variation in radial pressure along the height of the compact that is likely to result in a density gradient.

The combination of both higher residual radial stresses and a higher coefficient of friction at the powder-die wall interface for the unlubricated Ti powder resulted in a higher ejection force when compared with the lubricated Fe powder.

References

1. R.N. Caron and J.T. Staley, Effects of Composition, Processing, and Structure on Properties of Nonferrous Alloys, *ASM Handbooks Online, Vol. 20, Materials Selection and Design*, ASM International Metals Park, OH, 2004
2. F.H. Froes, S.J. Mashl, V.S. Moxson, J.C. Hebeisen, and V.A. Duz, The Technologies of Titanium Powder Metallurgy, *JOM*, 2005, **56**(11), p 46–48
3. M. Yousuff and N.W. Page, Die Stress and Internal Friction during Quasi-static and Dynamic Powder Compaction, *Powder Technol.*, 1993, **76**(3), p 299–307
4. B.J. Briscoe and S.L. Rough, The Effects of Wall Friction in Powder Compaction, *Colloid Surf. A-Physicochem. Eng. Asp.*, 1998, **137**(1–3), p 103–116
5. S. Turenne, C. Godère, Y. Thomas, and P.-É. Mongeon, Evaluation of Friction Conditions in Powder Compaction for Admixed and Die Wall Lubrication, *Powder Metall.*, 1999, **42**(3), p 263–268
6. D.M.M. Guyoncourt, J.H. Tweed, A. Gough, J. Dawson, and L. Pater, Constitutive Data and Friction Measurements of Powders using Instrumented Die, *Powder Metall.*, 2001, **44**(1), p 25–33
7. N. Solimanjad and R. Larsson, Die Wall Friction and Influence of Some Process Parameters on Friction in Iron Powder Compaction, *Mater. Sci. Technol.*, 2003, **19**(12), p 1777–1782
8. S. Strijbos, P.J. Rankin, R.J. Klein Wassink, J. Bannink G.J. Oudemans, Stress Occurring During One-sided Die Compaction of Powders, *Powder Technol.*, 1977, **18**(2), p 187–200
9. E. Pedersen, Model for Powder Compression which takes Diewall Friction into Account, *Powder Technol.*, 1986, **45**(2), p 155–157
10. D.T. Gethin, A.K. Ariffin, D.V. Tran, and R.W. Lewis, Compaction and Ejection of Green Powder Compacts, *Powder Metall.*, 1994, **37**(1), p 42–52
11. Y.S. Kwon, H.T. Lee, and K.T. Kim, Analysis for Cold Die Compaction of Stainless-Steel Powder, *J. Eng. Mater. Technol. Trans. ASME*, 1997, **119**(4), p 366–373
12. T. Canta and D. Frunza, Friction-assisted Pressing of PM Components, *J. Mater. Process. Technol.*, 2003, **143–144**, p 645–650
13. A.J. Matchett and T. Yanagida, Elastic Modulus of Powder Beds – The Effects of Wall Friction: A Model Compared to Experimental Data, *Powder Technol.*, 2003, **137**(3), p 148–158